Cooperative Synthesis of Control and Display Augmentation in Approach and Landing

Sanjay Garg* and David K. Schmidt†
Purdue University, West Lafayette, Indiana 47907

Application of the cooperative methodology to synthesize control/display augmentation systems for the piloted longitudinal landing task with a modern, statically unstable, fighter aircraft is considered. Starting with a control augmentation law that yields augmented vehicle dynamics that meet level I handling qualities specifications, the effect of time delay in the head-up display is studied using model-based criterion. This evaluation showed that even with "good" conventional dynamics, a realistic value of display time delay will cause significant deterioration in pilot workload and piloted-system performance. Application of the cooperative methodology to control augmentation alone resulted in augmented vehicle dynamics which provide direct control of the flight path from the pilot stick. Analytical evaluation of these dynamics indicates that such dynamics might lead to improved pilot ratings over conventional vehicle dynamics, especially in the presence of time delays in the system. Also, application of the methodology to simultaneous synthesis of control augmentation and flight director laws revealed that it might be advantageous to consider the control/display tradeoff in the early design stages.

Introduction

THE importance of considering the interaction between display sophistication and control system complexity in the design of manually controlled systems has been pointed out in various studies (see for example Refs. 1 and 2). Recently, a methodology called the cooperative methodology[3,4] has been presented that is intended to provide a systematic approach to synthesizing pilot-optimal control and display augmentation in complex, closed-loop manual control tasks. The major advantage of the cooperative methodology is clearly in terms of its applicability to modern flight vehicles exhibiting unconventional dynamics. Therefore, as an important step in the overall development of the methodology, its application to the synthesis of control/display augmentaiton for an unstable vehicle in a complex, piloted task was considered. In this paper, the characteristic results from this application of the methodology are presented along with the detailed analytical evaluations of the synthesized designs.

In the following, the characteristic dynamics of the vehicle being considered are first discussed. The vehicle has unstable bare-airframe dynamics, so several control laws will be synthesized for augmenting the airframe dynamics. First, an augmentation control law based on conventional design techniques is presented as a baseline case for later comparison with the cooperative-synthesis designs. The baseline conventionally augmented vehicle dynamics are based on existing handling qualities specifications[5] and are evaluated by comparison with systems flight tested in a previous experimental study.

An analytical procedure for evaluating the handling qualities of flight vehicles in the piloted approach and landing task is then presented. This procedure is based on an optimal control model (OCM) of human behavior[6] and is quite similar to that used in a previous study.[7] A head-up display (HUD) is assumed to be available to the pilot for the landing task. Model-based evaluation results are discussed for the conventionally augmented vehicle in the short takeoff and landing (STOL) approach task.

In general, when considering HUDs, some display dynamics will be introduced due to the processing of raw data from the aircraft sensors to obtain the information to be displayed on the HUD. These dynamics will essentially be band-limited filters and time delays. The effects of display dynamics on pilot performance and workload was studied in Ref. 8 by conducting man-in-the-loop simulations for generic plants, and the ability to predict these effects using the model-based techniques was demonstrated in Ref. 9. More recently, results from an in-flight evaluation of the effects of HUD dynamics on fighter aircraft flying qualities, reported in Ref. 10, indicate that added time delay in the display can lead to considerable deterioration in pilot rating. In the context of these findings, it was considered important to first quantify the effect of time delay in the HUD for the baseline conventionally augmented vehicle. An analytical investigation conducted for this purpose is also presented.

For a HUD with sufficient time delay to cause significant deterioration in piloted-system performance, three cases resulting from application of the cooperative methodology are then considered. These are systems that were designed to compensate for the effects of time delay present in the HUD. These cases are as follows:

1) Display augmentation alone: a flight director synthesized for the conventionally augmented vehicle with a HUD, including time delay.

2) Control augmentation only: a feedback augmentation system, augmenting the bare-airframe dynamics, but obtained via the cooperative methodology assuming a HUD with time delay. The objective here is to see whether the augmented system dynamics obtained by application of the cooperative methodology will be different from the conventionally augmented vehicle dynamics.

Received June 17, 1988; presented as Paper 88-4182 at the AIAA Guidance, Navigation and Control Conference, Minneapolis, MN, August 15-17, 1988; revision received Dec. 21, 1988.

*Doctoral Candidate, School of Aeronautics and Astronautics; currently, Controls Engineer, Sverdrup Technology, Inc., Lewis Research Center Group, Cleveland, OH 44130. Member AIAA.

†Professor; currently, Professor, Department of Mechanical and Aerospace Engineering, University of Arizona, Tempe, AZ. Associate Fellow AIAA.

3) Simultaneous control/display synthesis: a simultaneously synthesized control augmentation law and a flight director law, again, starting with the bare-airframe dynamics and a HUD with time delay. The objective here is to see whether considering the control/display trade-off in the early stages of design will lead to "better" results than those obtained for the preceding two cases.

The problem formulation for the three cases involving application of the cooperative methodology are presented and the characteristics of the synthesized systems are analyzed. Detailed model-based evaluation results for the piloted approach and landing task with these synthesized systems are then presented.

Vehicle Dynamics and Conventional Control Design

The vehicle considered is a STOL aircraft, with an airframe representative of a modern fighter aircraft. The linearized dynamics model for the longitudinal axis includes the three rigid-body degrees of freedom. The trim values for the landing-approach flight condition are $V_{app} = 202$ ft/s and $\gamma_0 = -3$ deg. The control effectors to be used are the horizontal tail (elevator) deflection, the thrust vector angle for a two-dimensional nozzle, the trailing-edge flap deflection, and thrust reversing, or

$$\bar{u} = [\delta_H, \delta_{TV}, \delta_F, K_{TR}]^T$$

where

δ_H = horizontal tail deflection, deg
δ_{TV} = thrust vector angle, deg
δ_F = trailing-edge flap deflection, deg
K_{TR} = thrust reverser, % flow split

The state vector for the vehicle model is

$$\bar{x}_v = [u, w, q, \theta]^T$$

where

u = forward speed, ft/s
w = vertical speed, ft/s
q = pitch rate, deg/s
θ = pitch angle, deg

The vehicle responses of interest are

$$\bar{y} = [u, \alpha, q, \theta, \gamma]^T$$

where

α = angle of attack, deg
γ = flight-path angle, deg

The vehicle dynamics can be written in the form

$$\dot{\bar{x}}_v = A_v \bar{x}_v + B_v \bar{u}$$

$$\bar{y} = C_v \bar{x}$$

The numerical values for the open-loop system matrices A_v, B_v, and C_v are listed in the Appendix.

Note that δ_H and δ_{TV} are effective in pitch control, δ_F is a direct lift device, and K_{TR} is effective in speed control. The key transfer functions for the vehicle then are as listed in Table 1.

The open-loop vehicle is unstable as seen from the roots of the open-loop characteristic polynomial $[D(s)]$ listed in Table 1. One way to synthesize the necessary augmentation is to require that the augmented vehicle dynamics meet the existing handling qualities specifications.[5] These specifications are

Table 1 Key transfer functions for STOL vehicle

$\{K(1/\tau)[\zeta,\omega_N] = K(s+1/\tau)(s^2+2\zeta\omega_N s+\omega_N^2)\}$
$D(s) = [0.62;\ 0.25]\ (-0.853)\ (1.535)$
$N^q_{\delta_H} = -1.763\ (0)\ (-0.040)\ (0.493)$
$N^q_{\delta_{TV}} = -1.432\ (0)\ (-0.075)\ (0.492)$
$N^\alpha_{\delta_F} = -0.101\ (-1.706)\ [0.51;\ 0.33]$
$N^u_{K_{TR}} = -0.294\ (0.069)\ (-1.27)\ (1.73)$

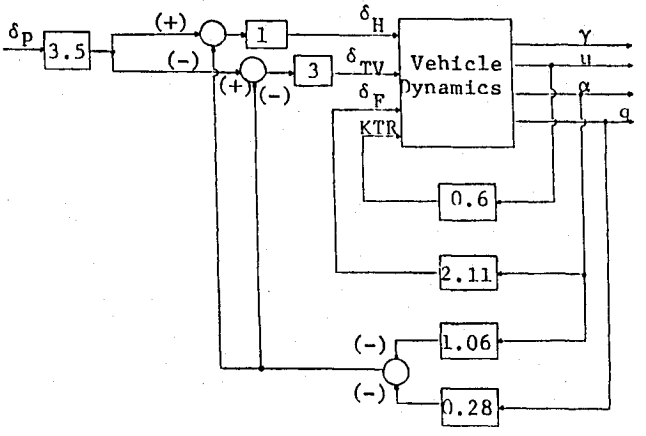

Fig. 1 Block diagram for conventional control augmentation.

based on flight vehicles exhibiting "classical" airplane-like modes (i.e., the short period and the phugoid mode). Another objective in synthesizing the control augmentation is to avoid excessive control deflections and rates.

Several approaches are available to the control system designer to design a control law such that the augmented vehicle will meet the handling qualities specifications. The conventional approach, consisting of considering appropriate sequential single-input/single-output loop closures based on the knowledge of the physical aspects of the problem was used to design the baseline control law. An excellent discussion of this approach can be found, for example, in Ref. 11. The block diagram for the conventional design is shown in Fig. 1. The steps involved in the conventional design are discussed in detail in Ref. 12.

The control augmentation being considered for the vehicle under study can be represented in a generic multi-input/multi-output block diagram form as shown in Fig. 2. Comparing Fig. 1 with Fig. 2, the values for the feedback gain matrix K and the effective control blending gains $(P \cdot k_\delta)$ from the pilot stick input that correspond to the conventional design are as follows:

$$K = \begin{bmatrix} 0 & -1.06 & -0.28 & 0 \\ 0 & -3.18 & -0.84 & 0 \\ 0 & -2.11 & 0 & 0 \\ -0.6 & 0 & 0 & 0 \end{bmatrix}, \quad P \cdot k_\delta = \begin{bmatrix} -3.5 \\ -10.5 \\ 0 \\ 0 \end{bmatrix} \tag{2}$$

In the rest of this paper, the augmented vehicle dynamics corresponding to the block diagram of Fig. 1 will be referred to as CD (baseline conventional design). The transfer functions from the pilot stick input to vehicle responses of interest for CD dynamics are listed in Table 2. The time histories for a unit step pilot input ($\delta_p = 1$ in.) are shown in Fig. 3. These results clearly indicate that the augmented vehicle exhibits "classical" short-period and phugoid characteristics. The level

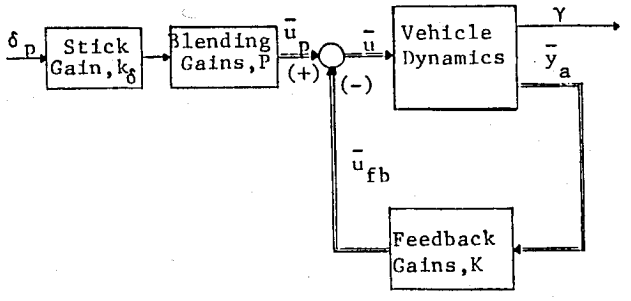

Fig. 2 Multi-input/multi-output control augmentation block diagram.

Table 2 Transfer functions for CD

$\{K(1/\tau)[\zeta,\omega_N] = K(s+1/\tau)(s^2+2\zeta\omega_N s+\omega_N^2)\}$
$D(s) = [\zeta_{ph};\ \omega_{ph}]\ [\zeta_{sp};\ \omega_{sp}]$
$= [0.54;\ 0.11]\ [0.64;\ 2.50]$
$N_{\delta_p}^{u} = -0.118\ (0.192)\ (3.452)\ (87.82)$
$N_{\delta_p}^{\alpha} = 0.826\ [0.65;\ 0.197]\ (25.68)$
$N_{\delta_p}^{q} = 21.21\ (0)\ (0.096)\ (0.74)$
$N_{\delta_p}^{\gamma} = -0.826\ (0.055)\ (-3.75)\ (3.96)$

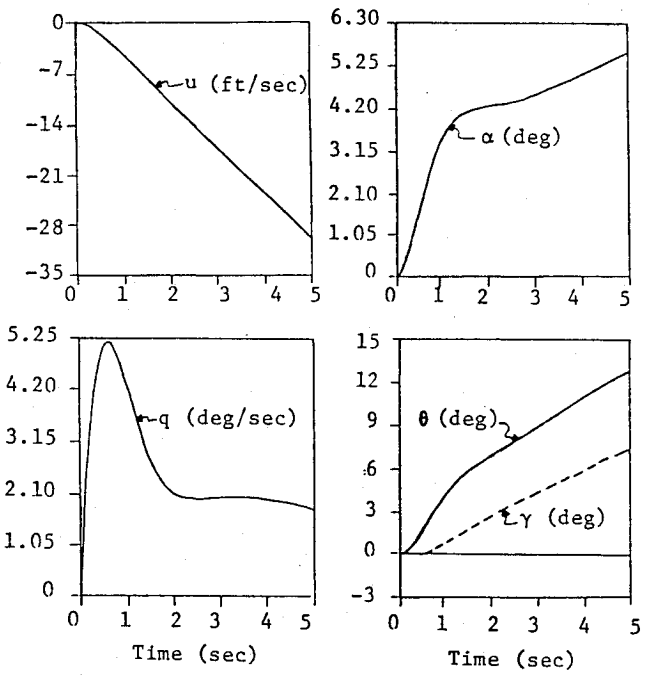

Fig. 3 CD system response for step pilot input ($\delta_p = 1$ in.).

I handling qualities requirements, from Ref. 5, are that $n_z/\alpha \geq 2.7$ g/rad, $0.35 < \zeta_{sp} < 1.3$, and that ω_{sp} be within a specified region depending on the actual value of n_z/α. For the CD dynamics, $n_z/\alpha = 4.5$ g/rad, and the level I boundaries for ω_{sp} are $0.8 < \omega_{sp} < 4.0$ rad/s. The CD dynamics satisfy the level I requirements for the short-period mode, as seen from Table 2, and also the phugoid mode is stable.

In Ref. 13, results are reported from an in-flight study conducted to evaluate the effects of control system dynamics on fighter flying qualities for the approach and landing task. One of the configurations evaluated in that study, and referred to as LAHOS (Landing and Approach of High Order Systems) 2-1 in the rest of this paper, consisted of just the classical short-period and phugoid modes with $\omega_{sp} = 2.29$ rad/s and $\zeta_{sp} = 0.59$. These short-period mode values are quite close to those for the CD dynamics, and also the transfer functions from the pilot stick input to vehicle responses of interest for LAHOS 2-1 [available in Ref. 13] were quite similar to those for the CD dynamics. The configuration LAHOS 2-1 was given a pilot rating of 2 on the Cooper-Harper scale.[14] Thus, it is conjectured that the conventionally designed augmented vehicle will also be rated level I in the approach and landing task, barring any control effector deflection and/or rate limiting.

Model-Based Evaluation and Head-Up Display Time-Delay Effects

Modeling Procedure

An extensive model-based study of the pilot/vehicle interaction in the approach and landing task was performed by Anderson and Schmidt.[7] In that study, it was hypothesized that the ability to precisely control flight-path angle is a necessary condition to obtain good pilot ratings in the approach, flare, and landing task. Under such a hypothesis, the pilot's task is modeled as tracking a (fictitious or pilot generated) flight-path-angle command and the configurations considered in the LAHOS study[13] were evaluated using the OCM. As shown in Ref. 7, this procedure led to excellent correlation between pilot ratings and model results, such as pilot phase compensation and closed-loop rms flight-path error. A similar modeling approach will be used in the present study.

In the formulation of the optimal control modeling approach,[6] the task of precisely tracking a flight-path-angle command is represented by selecting the following objective function:

$$J_p = E\left\{\lim_{T\to\infty}\frac{1}{T}\int_0^T(\gamma_e^2 + g_p\delta_p^2)\,dt\right\} \tag{3}$$

where γ_e is the flight-path tracking error ($\gamma_e = \gamma_c - \gamma$) and g_p is selected to yield a reasonable pilot "controller" bandwidth, which is reflected in the value of the neuromotor lag time constant τ_N. As in Ref. 7, a prefilter driven by "white" noise was used to generate a hypothesized flight-path-angle command signal, with a frequency content representative of that required in a visual flight rule (VFR) landing task. The command dynamics were such that $\gamma_c = 3.25$ deg rms, and the signal bandwidth was 0.5 rad/s.

A HUD was assumed to be available to the pilot. A detailed example of an operative HUD may be found in Ref. 15. Within the framework of the task being modeled, that of precise control of flight-path angle, the pilot's observation for a HUD without a flight director signal (the case with the flight director will be discussed later), was taken as follows:

$$\bar{y}_{p_{\text{HUD}}} = [\gamma_e,\ \dot{\gamma}_e,\ \gamma,\ \dot{\gamma},\ \theta,\ \dot{\theta}]^T \tag{4}$$

If a time delay τ_d s is present in the HUD symbology, the pilot's observations are given by

$$\bar{y}_{p_{\text{HUD}+\tau_d}} = \bar{y}_{p_{\text{HUD}}}(s)e^{-\tau_d s} \tag{5}$$

where $\bar{y}_{p_{\text{HUD}}}$ is as defined in Eq. (4). Within the framework of the OCM, the time delay can be accounted for in terms of a Pade approximation. If it is assumed that the pilot derives all the information relevant to the task from the HUD, the time delay can be reflected at the plant input, to obtain an equivalent system. The delayed input δ is given by

$$\delta = \delta_p e^{-\tau_d s} \tag{6}$$

This approach was used to assess the effects of HUD time delay.

The remaining model parameters were set to reasonable

Table 3 CD system performance

Classification	τ_N, s	rms γ_e, deg	rms γ, deg	rms θ, deg	rms q, deg/s	rms u, ft/s	rms $\dot{\delta}_p$, in./s	J_p
2-1[a]	0.14	0.51	3.21	4.61	3.50	19.8	3.49	0.3
HUD	0.14	0.57	3.20	5.16	3.82	14.8	3.73	0.3
HUD + $\tau_d = 0.1$	0.19	0.69	3.17	5.13	3.68	14.7	2.49	0.5
HUD + $\tau_d = 0.2$	0.26	0.83	3.11	5.04	3.44	14.1	1.65	0.8

[a]LAHOS 2-1 results for ideal HUD.

"standard" values available in the literature. These are as follows:

1) Observation thresholds for angular deflections and angular rates were 0.05 deg and 0.18 deg/s—consistent with the choice in Ref. 7.

2) The "full attention" observation noise-to-signal ratio was chosen to be -20 dB for each observation based on results reported in Ref. 16.

3) The pilot's full attention was assumed to be devoted to the control task, with the attention allocation between the various observations optimized using the procedure in Ref. 17. For the attention optimization, the angular deflection and rate observations were considered in pairs (see Ref. 17).

4) A motor noise ratio of -25 dB as in Ref. 7.

5) The pilot's internal observation time delay of $\tau_p = 0.2$ s.

With the modeling procedure just discussed, the configuration CD was initially evaluated for the ideal HUD (no time delay) case and with g_p [see Eq. (3)] selected to yield $\tau_N = 0.1$ s as in Ref. 7. The pilot dynamics resulting from this modeling assumption were found to be unstable. Such a behavior implies a high bandwidth controller, probably beyond the capabilities of any human operator. Previous experimental studies[8,18] have shown that, when faced with an extremely difficult task, the pilot will be willing to accept degradation in performance in order to keep his workload within acceptable limits. In Ref. 9 it was shown that such a performance/workload tradeoff can be modeled using the OCM by a model-based adjustment of the neuromuscular lag time constant τ_N. This model-based τ_N adjustment procedure consists of plotting the normalized model performance [$\text{rms}(\gamma_e/\gamma_e|_{\tau_N=0.1})$] vs the normalized workload [$\text{rms}(\dot{\delta}_p/\dot{\delta}_p|_{\tau N}=0.1)$] as a function of τ_N. (Here, the rms value of the pilot control rate activity ($\dot{\delta}_p$) is used as a measure of workload based on the results reported in Ref. 19.) As the value of τ_N is increased from 0.1 (or the pilot model bandwidth is decreased), initially there will be significant reduction in workload with little perceptible degradation in performance until a value of τ_N is reached beyond which the performance will start degrading sharply for slight increases in τ_N. Thus, assuming that the well-trained pilot would work just hard enough to achieve an acceptable level of performance, the point on the curve at which the degradation in performance begins to be perceptible (the "knee" in the curve) can be considered to be the solution to the performance/workload trade-off made by the pilot. An example of this τ_N adjustment procedure is also available in Ref. 12. For all of the model-based evaluation results presented in this study, the τ_N adjustment procedure was used to obtain models of pilot behavior.

Model-Based Evaluation Results

The time-domain results in terms of rms tracking error γ_e, other vehicle responses of interest, and pilot control activity are listed in Table 3 for the CD vehicle dynamics. (The time-delay cases, also listed in Table 3, will be discussed later in this section.) The corresponding results for the LAHOS 2-1 configuration are also listed in Table 3. (Note that the results for LAHOS 2-1 configuration are different from those in Ref. 7 because of the different perception modeling procedure used in this analysis.) The values of τ_N obtained from the performance/workload analysis which correspond to these results are also listed.

Frequency-domain analysis is also of fundamental importance in understanding the pilot/vehicle/display interaction. Using the OCM, the pilot's control input can be represented as a linear combination of the effective pilot transfer functions for all the direct observations. The pilot input corresponding to the observations listed in Eq. (4) will be

$$u_p(s) = P_{\gamma_e}(s)\gamma_e(s) + P_{\gamma}(s)\gamma(s) + P_{\theta}(s)\theta(s) \tag{7}$$

In Eq. (7), the angular rate terms ($\dot{\gamma}_e$, $\dot{\gamma}$, $\dot{\theta}$) are not explicitly included because these are not direct observations and are assumed to be generated internally by the pilot from the corresponding angular deflection observations. The pilot (model) from Eq. (7) is multivariable, so it is not possible to directly identify the pilot's phase compensation that can be used as a measure of workload. However, exploiting the flight path to pitch attitude (γ/θ) characteristics of the dynamics under study, and carrying out some simple block diagram manipulation as in Ref. 7, an equivalent single-input/single-output pilot control input transfer function can be obtained as

$$u_p(s) = P_{\text{eq}}(s)\gamma_e(s) \tag{8}$$

This equivalent pilot model approach was used to evaluate the designs in this paper.

Table 4 CD frequency-domain results

Classification	G.M., dB	P.M., deg	ω_c, rad/s	$\measuredangle$ peq, deg
2-1[a]	2.4	23	2.1	46.2
HUD	2.5	23	1.9	28.8
HUD + $\tau_d = 0.1$	2.4	23	1.7	38.8
HUD + $\tau_d = 0.2$	2.4	23	1.5	50.1

[a]LAHOS 2-1 results for ideal HUD.

The model-based frequency domain results that are of interest are listed in Table 4 for the CD dynamics and for the LAHOS 2-1 configuration. The frequency-domain results consist of loop quality measures such as crossover frequency (ω_c), gain margin (G.M.), and phase margin (P.M.), which are defined in Fig. 4, for example, and maximum equivalent pilot-phase compensation [$\measuredangle \text{peq} \triangleq$ maximum of $\measuredangle P_{\text{eq}}(j\omega)$ in the crossover region, defined in Fig. 5] as a frequency-domain measure of workload. Figures 4 and 5 will be discussed further, later in this section.

The model results showed almost all attention being allocated to the flight-path error γ_e indicating that with flight-path information directly available to the pilot, the pitch attitude loop closure might be less important.

Comparing the results for CD dynamics with those for LAHOS 2-1 configuration, we note that both the time- and frequency-domain results are very similar. In fact $\measuredangle$ peq is slightly lower for CD dynamics, indicating that this configuration might result in a lower workload. As stated earlier, LAHOS 2-1 was rated level I in the flight experiments reported in Ref. 13; the closed-loop pilot/vehicle analysis results indicate that CD dynamics should be at least equally good.

The model-based results for the CD dynamics with HUD time delays of 0.1 and 0.2 s are also listed in Tables 3 and 4 to provide a comparison with the case of the ideal HUD (no time delay). From these tables, we note that HUD time delays result in deterioration in tracking performance and an increase in pilot workload ($\measuredangle$ peq). The pilot/vehicle open-loop transfer

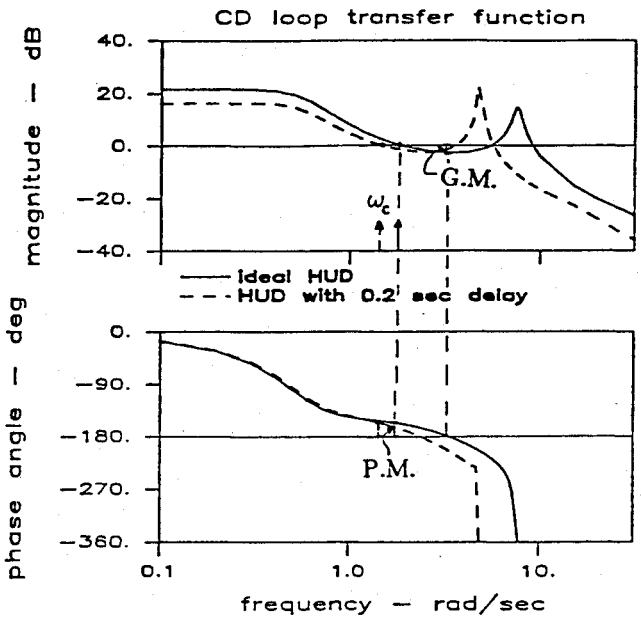

Fig. 4 Effect of HUD delay on pilot/vehicle loop transfer function $[(\gamma/\gamma_e)(j\omega)]$.

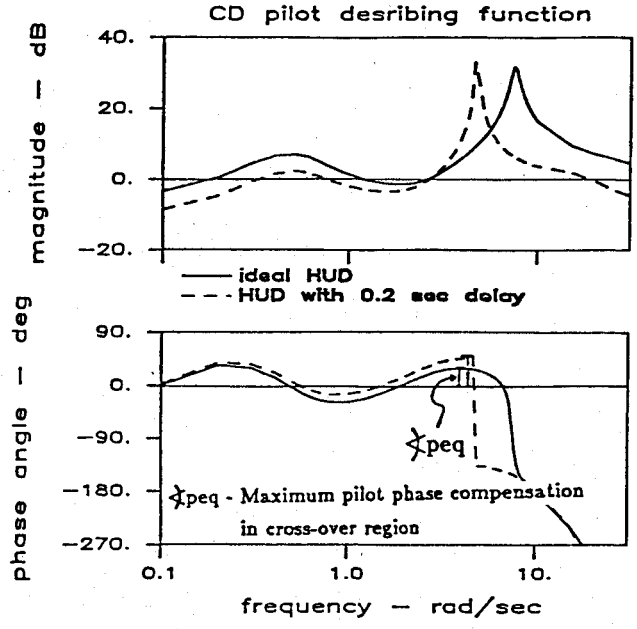

Fig. 5 Effect of HUD delay on pilot compensation $[P_{eq}(j\omega)]$.

functions $[(\gamma/\gamma_e)j\omega]$ for the ideal HUD and for the case with HUD delay $\tau_d = 0.2$ s are compared in Fig. 4, and the equivalent pilot describing functions are compared in Fig. 5. The reduction in cross-over frequency (ω_c) due to HUD time delay, as seen from Fig. 4, is consistent with experimentally measured results reported in Ref. 20. Figure 5 clearly shows the increase in required pilot phase-lead compensation due to HUD time delay.

In Ref. 7, the model-based performance (rms γ_e) was plotted against the model-based workload ($\measuredangle$ peq) for the various LAHOS configurations, and a correlation was obtained between the pilot ratings for a given configuration and its relative location on the performance/workload chart. Using similar evaluation criteria, the results for all the CD and LAHOS 2-1 configurations considered thus far in the analysis are shown in

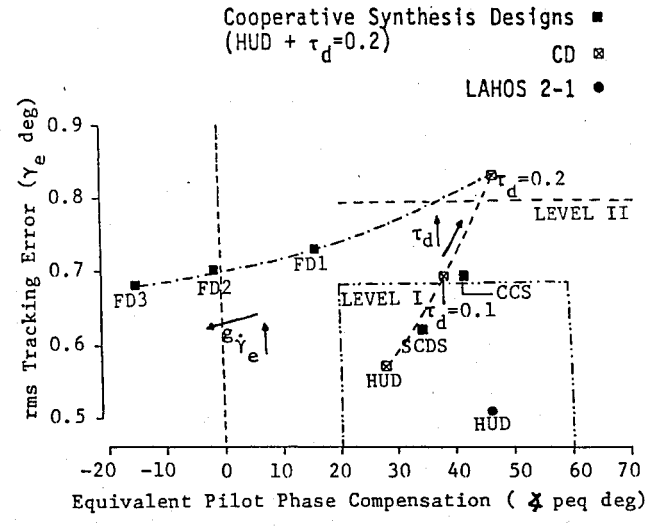

Fig. 6 Model-based performance/workload results for cooperative synthesis designs.

Fig. 6. (The configurations marked FD1, FD2, FD3, CCS, and SCDS in Fig. 6 are cooperative-synthesis designs, and these will be discussed later in this paper.) The handling-qualities-level boundaries obtained in Ref. 7 are also shown in Fig. 6. Although the boundaries obtained in Ref. 7 might not be directly applicable because of the differences in the modeling procedure, the trends in Fig. 6 do indicate that the CD dynamics will be level I with an ideal HUD.

The time-delay performance/workload results for CD dynamics indicate that for low values of time delay in the HUD, there will be little deterioration in pilot rating. This result is in agreement with experimental results reported in Ref. 10. But, for the case of $\tau_d = 0.2$ s, the deterioration in performance and workload is quite significant, which will probably result in the system handling qualities being rated level II or worse.

Cooperative Synthesis Application

The results obtained in the preceding section indicate that, for the CD vehicle dynamics, a HUD time delay of 0.2 s will considerably increase tracking error as well as pilot workload. One way of avoiding this is to provide a flight director on the HUD, designed to provide the pilot with lead information. Another way is to consider other augmented vehicle dynamics that are more suitable for the control task with HUD time delay. In this section, then, application of the cooperative methodology to control/display augmentation synthesis for the STOL vehicle with a HUD time delay of 0.2 s will be discussed. The problem formulation for the three augmentation cases to be considered is first presented and the characteristics of the resulting augmented systems are analyzed. The detailed model-based evaluation results for these augmented systems in the landing task are then presented.

Display Augmentation Alone

Application of the cooperative methodology to the design of a flight director (FD) law, with the CD vehicle dynamics, was considered first. The block diagram for display augmentation is as shown in Fig. 7. Based on the work reported in Refs. 21 and 22, the flight director signal was chosen to be of the form

$$\mathrm{FD} = \gamma_e + g_{\dot{\gamma}_e}\dot{\gamma}_e + g_\theta\theta + g_q q \qquad (9)$$

where $g_{(\,)}$ are the flight director gains to be determined; q and θ are included in Eq. (9) to account for the fact that the pilot might be closing the pitch attitude loop in the flight path tracking task. The $\dot{\gamma}_e$ is included to provide lead information. Note that when implementing a flight director of the form in

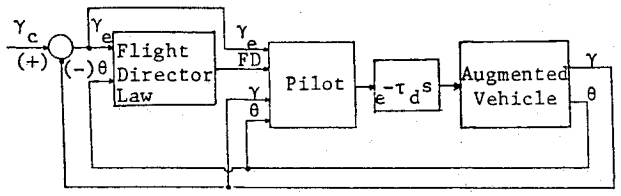

Fig. 7 Block diagram for flight director design.

Eq. (9), the pitch attitude signal would also be "washed-out" such that the flight director signal will approach γ_e in steady flight. The wash-out filter will not be considered in this analysis, however. In compact form, Eq. (9) can be written as

$$\mathrm{FD} = \gamma_e + G_d \bar{y}_d$$

with

$$\bar{y}_d = [\dot{\gamma}_e, \theta, q]$$

and $G_d = [g_{\dot{\gamma}_e}, g_\theta, g_q]^T$.

If the flight director signal is displayed to the pilot through an additional first-order lag at, say, 100 rad/s, then

$$\mathrm{FD}(s) = \frac{100(\gamma_e + G_d \bar{y}_d)}{(s+100)} \tag{10}$$

This display augmentation of Eq. (10) can be represented within the framework of the cooperative methodology[3,4,12] as

$$\dot{\mathrm{FD}} = -100\,\mathrm{FD} + 100\gamma_e + 100u_d \tag{11}$$

with the display control law defined as $u_d = G_d \bar{y}_d$.

The pilot's observations with the flight director on the HUD are taken as

$$\bar{y}_{\mathrm{FD}} = [\gamma_e, \dot{\gamma}_e, \gamma, \dot{\gamma}, \theta, \dot{\theta}, \mathrm{FD}, \dot{\mathrm{FD}}]^T \tag{12}$$

The cost function J_1 for the pilot (model) is

$$J_1 = J_p = E\left\{\lim_{T\to\infty} \frac{1}{T}\int_0^T (\gamma_e^2 + g_p \dot{\delta}_p^2)\,\mathrm{d}t\right\} \tag{13}$$

Note that even with the flight director, the pilot's task, in the synthesis as well as for model-based evaluation, is modeled as that of tracking the flight-path command rather than the flight director signal. This modeling approach is consistent with the results of the study reported in Ref. 23.

The cost function to be minimized by the display control law u_d is

$$J_2 = J_p + E\left\{\lim_{T\to\infty} \frac{1}{T}\int_0^T (F_{2d} u_d^2)\,\mathrm{d}t\right\} \tag{14}$$

which is consistent with the desire to design a flight director signal to improve the pilot rating of the system. In Eq. (14), F_{2d} is a scalar determining the magnitude of the display gains. The requirements for the flight director design[21] are that the FD signal should be consistent with γ_e and that the flight director should not appear to be "busy" (i.e., FD rms value should not be too high). These requirements place qualitative constraints on the magnitude of the display control gains G_d.

Using the preceding formulation, cooperative display synthesis was performed for three values of F_{2d}. The F_{2d} values and the resulting gains G_d are listed in Table 5. For the purposes of further discussion, these three cases will be referred to as FD1, FD2, and FD3, respectively, in the order of decreasing F_{2d} or increasing gains. From Table 5, we note that the gains g_q and g_θ are ≈ 0 for all the three cases, indicating that no improvement in pilot performance or workload is to be obtained by incorporating θ or q information into the flight director. This result is consistent with the model-based attention allocation results obtained in the previous section, which showed that the pitch attitude loop closure is not too important in the flight-path tracking task with the HUD, which displays flight-path angle.

Table 5 Cooperative display synthesis results

Classification	F_{2d}	$g_{\dot{\gamma}_e}$	g_θ	g_q
FD1	2.0	0.18	0.0	−0.01
FD2	1.0	0.35	0.0	−0.02
FD3	0.5	0.57	0.0	−0.04

The complete model-based evaluation results for flight director cases FD1, FD2, and FD3 are discussed later in this paper.

Control Augmentation Only

In this section, application of the cooperative methodology to synthesis of an augmentation control law for the bare-airframe STOL vehicle, rather than flight director, will be discussed for the case including a HUD with a time delay of $\tau_d = 0.2$ s. The form of control augmentation to be considered is as shown in the block diagram of Fig. 2.

The cooperative synthesis procedure was set up such that the control blending gains (P in Fig. 2) could be obtained via the optimization process. The stick gain k_δ was, however, adjusted after the synthesis to yield reasonable values of control sensitivity. The control law consistent with Fig. 2 (with $k_\delta = 1$ for synthesis purposes) can be written as

$$\bar{u} = [-K \quad P] \begin{bmatrix} u \\ \alpha \\ q \\ \theta \\ \delta_p \end{bmatrix}$$

which results in the following definitions for the augmentation controller $\bar{u}_a$ within the framework of the cooperative methodology[3,4,12]

$$\bar{u}_a = \bar{u}, \qquad G_a = [-K, P], \qquad \bar{y}_a = [u, \alpha, q, \theta, \delta]^T \tag{15}$$

In Eq. (15), δ_p has been replaced by the delayed input δ [defined by Eq. (6)] to take the effect of HUD delay into account in the synthesis procedure.

The pilot's observations are now taken to be

$$\bar{y}_p = [\gamma_e, \dot{\gamma}_e, \gamma, \dot{\gamma}, \theta, \dot{\theta}]^T \tag{16}$$

The cost function to be minimized by the augmentation law u_a is now

$$J_2 = J_p + E\left\{\lim_{T\to\infty} \frac{1}{T}\int_0^T (\bar{u}_a F_2 \bar{u}_a)\,\mathrm{d}t\right\} \tag{17}$$

and J_p is as in Eq. (13). The weighting matrix F_2 in Eq. (17) was chosen to be of the form

$$F_2 = \mathrm{diag}\left[\frac{1}{u_{i_{\max}}^2}\right]$$

$$= \mathrm{diag}[0.01,\ 1.11e-03,\ 0.04,\ 4.0e-04] \tag{18}$$

with $u_{i_{\max}}$ corresponding to the maximum allowable control deflections.

The cooperative control synthesis numerical algorithm (described in Ref. 12) was initialized with an initial choice of augmentation gains [G_a in Eq. (15)] corresponding to $\delta_H = -\delta_p$. After the algorithm converged, the stick gain k_δ was

Table 6 Transfer functions for CCS dynamics

$\{K(1/\tau)[\zeta,\omega_N] = K(s+1/\tau)(s^2+2\zeta\omega_N s+\omega_N^2)\}$
$D(s) = (0.114)\ (1.159)\ [0.57;\ 1.48]$
$N_{\delta_p}^{u} = 0.260\ (0.125)\ (2.774)\ (-44.0)$
$N_{\delta_p}^{\alpha} = 0.338\ [0.82;\ 0.167]\ (77.37)$
$N_{\delta_p}^{q} = 27.63\ (0)\ (0.093)\ (0.542)$
$N_{\delta_p}^{\gamma} = -0.338\ (0.064)\ (3.82)\ (-7.93)$

adjusted such that the flight-path response sensitivity for the augmented vehicle dynamics corresponding to the convergent gains is comparable to the LAHOS 2-1 and the CD systems discussed earlier. For the remainder of this paper, these augmented vehicle dynamics will be referred to as CCS (cooperative control synthesis) dynamics. The feedback gains K and the effective control blending gains $P \cdot k_\delta$ corresponding to the CCS dynamics are as follows

$$K = \begin{bmatrix} 0.248 & -0.342 & -0.729 & -0.443 \\ 0.697 & -0.600 & -0.244 & -0.922 \\ -0.323 & 0.235 & 0.216 & 0.366 \\ -0.559 & 0.106 & -0.153 & 0.024 \end{bmatrix}$$

$$P \cdot k_\delta = \begin{bmatrix} -6.36 \\ -9.43 \\ 7.36 \\ -5.43 \end{bmatrix} \tag{19}$$

The transfer functions from the pilot input to vehicle responses of interest for the CCS dynamics are listed in Table 6, and the time histories for vehicle response to step pilot input ($\delta_p = 1$ in.) are shown in Fig. 8. From these results, it is clear that the CCS dynamics are very different from the "classical" longitudinal airplane modes such as those obtained for the CD configuration. Although the numerators for the vehicle responses are of the same form for the CCS and CD dynamics (as seen from Tables 6 and 2, respectively), there is no conventional phugoid mode in the CCS augmented system, which results in very different time histories from those for the CD system (seen by comparing Figs. 3 and 8).

From the time history and transfer function for γ, for the CCS dynamics, we note that the pilot stick deflection commands flight-path angle in the steady state. Flight-path command laws have been tested in various V/STOL research programs at the NASA Ames Research Center[24] and shown to be superior to attitude and attitude rate command laws. However, in the implementations for these studies (at NASA Ames), the pilots used a backside approach for landing, and the flight path was commanded via a thumbwheel on the throttle. Implementation of the flight-path command via the stick, as suggested here, might require some means of trim off-load logic so that the pilot does not have to continuously hold the stick at a constant deflection for commanding a step change in flight-path angle. The complete model-based evaluation results for the flight-path tracking task with these CCS dynamics are discussed later in this paper.

Simultaneous Control/Display Synthesis

Finally, the cooperative synthesis algorithm was applied to *simultaneously* synthesize a vehicle augmentation control law and a flight director for the STOL vehicle while still considering a HUD with a time delay of $\tau_d = 0.2$ s. The control formulation is as in the preceding section and the display augmentation formulation is as in the section previous to that, but the vehicle dynamics are now the bare-airframe dynamics.

The augmentation gains G_a, augmentation controller $\bar{u}_a$,

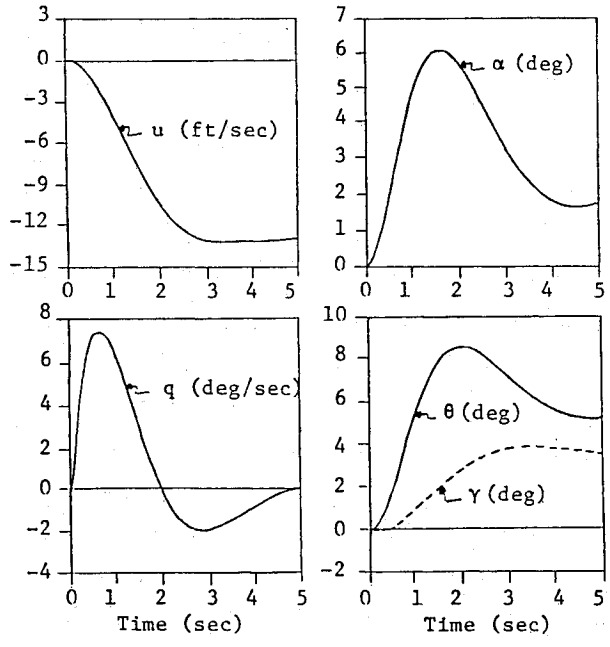

Fig. 8 CCS system response for step pilot input ($\delta_p = 1$ in.).

and measurements $\bar{y}_a$ for the augmentation controller are as in Eq. (15). Based on the earlier results, showing that pitch information is not used by the pilot in the control task once γ_e observation is directly available, the display controller was defined as follows:

$$y_d = \dot{\gamma}_e, \qquad G_d = g_{\dot{\gamma}_e}, \qquad u_d = G_d y_d$$

The cost functions were chosen to be J_p as in Eq. (11) and

$$J_2 = J_p + E\left\{\lim_{T\to\infty} \frac{1}{T}\int_0^T (F_{2d}u_d^2 + \bar{u}_a F_2 \bar{u}_a)\, dt\right\} \tag{20}$$

with F_2 as in Eq. (18) and $F_{2d} = 1$. The choice of F_2 is consistent with the hypothesized control deflection limits. As shown by later analysis, the choice $F_{2d} = 1$ led to a reasonable (in terms of consistency with the error γ_e) flight director for the case of display augmentation alone. So this value of F_{2d} was used for the simultaneous control/display synthesis.

The cooperative control/display synthesis numerical algorithm was exercised with the same initial control augmentation gains G_a as for the case of control augmentation only. The stick gain k_δ was again adjusted to yield a reasonable flight-path-angle response sensitivity for the augmented vehicle dynamics corresponding to the convergent gains. In the rest of the paper, this simultaneous control/display synthesis design will be referred to as SCDS design.

Corresponding to the block diagram of Fig. 2, the feedback gains K and the effective control blending gains $P \cdot k_\delta$ for the SCDS augmented vehicle are as follows, with the flight director gain $G_d = 0.25$:

$$K = \begin{bmatrix} 0.438 & -0.497 & -0.303 & -0.622 \\ 0.218 & -0.396 & -0.190 & -0.580 \\ -0.243 & 0.085 & 0.115 & 0.198 \\ -1.020 & 0.139 & -0.181 & 0.177 \end{bmatrix}$$

$$P \cdot k_\delta = \begin{bmatrix} -6.35 \\ -3.88 \\ 5.43 \\ -2.02 \end{bmatrix} \tag{21}$$

The transfer functions from the pilot input to the augmented vehicle responses of interest, for the SCDS system, are listed in Table 7. Comparing these results to those in Table 6, we note that the SCDS dynamics are quite similar to the CCS dynamics.

Model-Based Evaluation Results

The model-based evaluation results are listed in Tables 8 and 9 for the three cases of display augmentation (flight director) with CD dynamics (FD1, FD2, and FD3), the CCS vehicle dynamics (without flight director), and the SCDS system, using the modeling procedure discussed earlier. Table 8 shows the time-domain, piloted-system performance, and Table 9 shows the frequency-domain results of interest. The results for the CD dynamics without any flight director are also listed in these tables to provide a comparison with the cooperative synthesis designs. Note that all the results listed in Tables 8 and 9, including those for the CD dynamics without any flight director, are for a HUD with a time delay of 0.2 s.

First considering the cases FD1 to FD3, the time-domain performance results in Table 8 indicate that as the gain $g_{\dot{\gamma}_e}$ is increased, i.e, from FD1 to FD3 as in Table 5, the piloted-system performance will improve and so will the value of J_p. Compared to the case of no flight director (CD in Table 8), even the small value of $g_{\dot{\gamma}_e}$ in the FD1 case results in a significant improvement in tracking performance. However, the ratios of the rms values of FD and γ_e and the ratios of the corresponding rates [(FD/γ_e)rms and (FD/$\dot{\gamma}_e$)rms], also listed in Table 8, indicate that high values of $g_{\dot{\gamma}_e}$ could result in a "busy" flight director signal incompatible with the γ_e signal. Therefore, based on the experimental results reported in Ref. 12, the display augmentation FD3 will be undesirable even though the model-based values of J_p and rms γ_e indicate otherwise. The pilot phase compensation results for the cases with flight director (FD1, FD2, FD3, and SCDS), listed in Table 9, were obtained for the equivalent pilot-describing function reflected to the FD signal. The frequency-domain results for the cases FD1–FD3 indicate that providing a flight director significantly reduces required maximum pilot phase-lead compensation ($\measuredangle$ peq) and also results in a slight increase in loop cross-over frequency ω_c.

Considering the CCS dynamics next, we note from Table 8 that the tracking performance (γ_e rms) as well as the value of J_p for the CCS dynamics are much improved over those for the CD dynamics. Also the speed deviation (u rms) is much lower for the CCS dynamics, indicating that speed regulation might be easier when performing the landing task with such an augmented vehicle. However, the high-pitch deviations (both θ and q rms values) for the CCS dynamics might be excessive. The frequency-domain results for the CCS dynamics listed in Table 9 do show increased pilot/vehicle loop cross-over frequency and decreased pilot phase lead compensation when compared to corresponding results for the CD dynamics.

Finally, considering the SCDS system, the performance results in Table 8 do show much improved values of γ_e rms and J_p as compared to those for the CCS and FD2 cases. Also the speed deviations are much reduced and the pitch deviations are lower than the CCS case. The ratios of rms values FD and γ_e and associated rates are quite small, indicating consistency of flight director with the tracking error. The frequency-domain results listed in Table 9 show a slight increase in pilot/vehicle loop cross-over frequency and reduction in required pilot phase-lead compensation for the SCDS case as compared to the CCS case.

Although piloted-system control deflection rms values are not presented in this paper, an analysis of these results[12] showed that for the CCS and SCDS designs, the augmentation law was such that the rms deflections for all the controls (δ_H, δ_{TV}, δ_F, and K_{TR}) were less than the allowable maximum control deflections [values used to determine F_2 in Eq. (18)]. For the conventional CD, however, the rms flap deflection for the piloted system exceeded the allowable maximum deflection. These results indicate that the cooperative methodology has the capability to provide pilot-optimal control augmentation within other system constraints such as limits on control-surface deflections.

The performance/workload results for the cooperative synthesis designs (FD1–FD3, CCS, and SCDS) are also plotted in Fig. 6 in the format of the results reported in Ref. 7. From Fig. 6, we again note that providing a flight director results in significant reduction in pilot workload with limited improvement in performance, especially when compatibility constraints for the flight director signal (as discussed earlier) are taken into account. The close proximity of the SCDS system and the CD case for ideal HUD (no time delay) in Fig. 6 indicates that application of the cooperative methodology to simultaneous synthesis of control/display augmentation results in a system that compensates adequately for the HUD time delay of 0.2 s. Note that, as seen from Fig. 6, the overall performance/workload results for the SCDS system show im-

Table 7 Transfer functions for SCDS dynamics

$\left\{K(1/\tau)[\zeta,\omega_N] = K(s+1/\tau)(s^2+2\zeta\omega_N s+\omega_N^2)\right\}$

$D(s) = (0.147)\ (0.905)\ [0.40;\ 1.54]$

$N_{\delta_p}^{u} = -0.690\ (0.126)\ (2.782)\ (11.751)$

$N_{\delta_p}^{\alpha} = 0.233\ (0.048)\ (0.344)\ (76.46)$

$N_{\delta_p}^{q} = 18.35\ (0)\ (0.175)\ (0.606)$

$N_{\delta_p}^{\gamma} = -0.233\ (0.229)\ (4.645)\ (-6.674)$

$N_{\delta_p}^{FD} = -0.058\ (0.229)\ (\underline{4.02})\ (4.645)\ (-6.674)$

Table 9 Cooperative synthesis designs frequency-domain results (HUD + τ_d = 0.2)

Classification	G.M., dB	P.M., deg	ω_c, rad/s	$\measuredangle$ peq, deg
FD1	2.6	22	1.7	16.3
FD2	2.6	23	1.7	−1.0
FD3	2.6	22	1.8	−14.7
CCS	2.5	26	1.7	42.3
SCDS	2.3	25	1.8	34.5
CD[a]	2.4	23	1.5	50.1

[a]Conventional design (CD) results shown for comparison.

Table 8 Cooperative synthesis designs—system performance (HUD + τ_d = 0.2)

Classification	τ_N, s	rms γ_e, deg	rms γ, deg	rms θ, deg	rms q, deg/s	rms u, ft/s	rms $\dot{\delta}_p$, in./s	J_p	rms FD/γ_e	rms FD/$\dot{\gamma}_e$
FD1	0.26	0.73	3.14	5.07	3.30	14.4	1.56	0.70	1.01	1.10
FD2	0.26	0.70	3.15	5.08	3.25	14.4	1.52	0.64	1.06	1.41
FD3	0.26	0.68	3.15	5.08	3.22	14.5	1.50	0.61	1.18	1.95
CCS	0.22	0.69	3.15	6.27	5.42	11.7	2.13	0.62	—	—
SCDS	0.22	0.62	3.17	5.53	4.78	8.2	2.18	0.52	1.06	1.15
CD[a]	0.26	0.83	3.11	5.04	3.44	14.1	1.65	0.87	—	—

[a]Conventional design (CD) results shown for comparison.

provement over those for the CCS dynamics (obtained by cooperative *control* synthesis alone) as well as those for the FD2 case (reasonable flight director with CD dynamics obtained by cooperative *display* synthesis alone).

Summary and Conclusions

Application of the cooperative methodology to control/display design for tlhe piloted longitudinal landing task with a modern fighter aircraft was considered. The aircraft had unstable bare-airframe dynamics. An augmentation control law based on conventional design techniques was first developed to yield level I handling qualities vehicle dynamics consisting of "classical" longitudinal aircraft modes. Using model-based criterion with a modeling procedure similar to that developed in an earlier study of the longitudinal landing task, the effects of time delay in the head-up display were studied. This evaluation showed that even with "good" conventional dynamics, a realistic value of time delay would cause sufficient deterioration in pilot workload and piloted-system performance to result in worse than level I pilot rating.

Various cases of control/display augmentation in the presence of time delay in the head-up display were then considered using the cooperative methodology. Detailed model-based evaluations, using time- and frequency-domain measures, were performed for the resulting systems. Application of the cooperative methodology to display augmentation alone resulted in flight director laws that provide significant reduction in pilot workload. The analytical evaluation of these flight director laws confirmed previous findings that display augmentation provides only limited improvement in closed-loop performance of manually controlled systems. Application of the cooperative methodology to control augmentation only resulted in augmented vehicle dynamics that are very different from the conventional dynamics. These augmented vehicle dynamics provide direct control of flight path from the pilot stick. Model-based evaluation results indicate that such dynamics might lead to improved pilot rating even in the presence of time delay in the head-up display. Finally, application of the cooperative methodology to the simultaneous synthesis of control augmentation and flight director laws was considered. Model-based evaluation of the combination of control augmentation and flight director, obtained from the simultaneous control/display synthesis, indicates that this system will result in better piloted-system performance than for either the augmented vehicle dynamics obtained by considering control augmentation alone or the combination of conventional dynamics with a flight director. These results indicate that it might be advantageous to consider the control/display trade-off in the early design stages in order to obtain a good overall system.

Appendix

Vehicle System Matrices

The numerical values for the vehicle system matrices, defined in Eq. (1) are as follows:

$$A_v = \begin{bmatrix} -0.0575 & -0.2023 & -0.4656 & -0.5600 \\ -0.2900 & -0.3237 & 3.4399 & -0.0459 \\ -0.1727 & 0.3317 & -0.6121 & 0.0061 \\ 0.0 & 0.0 & 1.0 & 0.0 \end{bmatrix}$$

$$B_v = \begin{bmatrix} 0.1237 & -0.0299 & -0.1134 & -0.2940 \\ -0.3208 & -0.1701 & -0.3565 & -0.0298 \\ -1.7627 & -1.4325 & 0.2021 & -0.2481 \\ 0.0 & 0.0 & 0.0 & 0.0 \end{bmatrix}$$

$$C_v = \begin{bmatrix} 1.0 & 0.0 & 0.0 & 0.0 \\ 0.0 & 0.284 & 0.0 & 0.0 \\ 0.0 & 0.0 & 1.0 & 0.0 \\ 0.0 & 0.0 & 0.0 & 1.0 \\ 0.0 & -0.284 & 0.0 & 1.0 \end{bmatrix}$$

Acknowledgments

This research was supported in part under Grant NAG4-1 by NASA Dryden Research Facility, Ames Research Center, and in part by Honeywell Systems Research Center, Minneapolis, as a consulting subcontract on U.S. Air Force Flight Dynamics Laboratory Contract F33615-86-c-3615. Donald T. Berry was the contract monitor on the NASA grant. The authors would also like to thank the anonymous reviewers for their helpful suggestions.

References

[1]"V/STOL Displays for Approach and Landing, " AGARD Rept. 594, June 1972.

[2]Lebacqz, J. V., and Aiken, E. W., "Experimental Investigation of Control-Display Requirements for VTOL Instrument Transitions," *Journal of Guidance and Control,* Vol. 1, No. 4, 1978, pp. 261-268.

[3]Garg, S., and Schmidt, D. K., "Optimal Cooperative Control Synthesis of Active Displays," NASA CR-4085, June 1987.

[4]Garg, S., and Schmidt, D. K., "Cooperative Synthesis of Control and Display Augmentation," *Journal of Guidance, Control and Dynamics,* Vol. 12, No. 1, 1989, pp. 54-61.

[5]"Military Specification—Flying Qualities of Piloted Airplanes," Wright Patterson AFB, OH, MIL-F-8785C, Nov. 1980.

[6]Kleinman, D. L., Baron, S., and Levison, W. H., "An Optimal Control Model of Human Response," Pts. I and II, *Automatica,* Vol. 6, May 1970, pp. 357-383.

[7]Anderson, M. R., and Schmidt, D. K., "Closed-Loop Pilot Vehicle Analysis of the Approach and Landing Task," *Journal of Guidance, Control, and Dynamics,* Vol. 10, No. 2, 1987, pp. 187-194.

[8]McCormack, L. B., and George, F. L., "Effect of Varying Cockpit Display Dynamics on Pilot Workload and Performance," *Proceedings of the 22nd Annual Conference on Manual Control,* Air Force Wright Aeronautics Lab., Wright Patterson AFB, OH, AFWAL-TR-86-3093, Dec. 1986.

[9]Garg, S., and Schmidt, D. K., "Model-Based Evaluation of Display Dynamics Effects in Pursuit Tracking," *Proceedings of the 22nd Annual Conference on Manual Control,* Air Force Wright Aeronautics Lab., Wright Patterson AFB, OH, AFWAL-TR-86-3093, Dec. 1986.

[10]Bailey, R. E., "Effect of Head-Up Display Dynamics of Fighter Flying Qualities," AIAA Paper 86-2206, Aug. 1986.

[11]McRuer, D. T., Ashkenas, I., and Graham, D., *Aircraft Dynamics and Automatic Control,* Princeton Univ. Press, Princeton, NJ, 1973.

[12]Garg, S., "Model-Based Analysis and Cooperative Synthesis of Control and Display Augmentation for Piloted Flight Vehicles," Ph.D. Thesis, School of Aeronautics and Astronautics, Purdue University, West Lafayette, IN, May 1988.

[13]Smith, R. E., "Effects of Control System Dynamics on Fighter Approach and Landing Longitudinal Flying Qualities," Air Force Flight Dynamics Lab., Wright Patterson AFB, OH., AFFDL-TR-78-122, March 1978.

[14]Cooper, G. E., and Harper, R. P., Jr., "The Use of Pilot Rating Scale in the Evaluation of Aircraft Handling Qualities," NASA TN-D-5153, April 1969.

[15]"HUD Guidance Improves Landing Performance," *Aerospace Engineering,* July 1987.

[16]Levison, W. H., "The Effects of Display Gain and Signal Bandwidth on Human Controller Remnant," Aerospace Medical Research Lab., Wright-Patterson AFB, OH, AMRL-TR-70-93, March 1971.

[17]Hoffman, W. C., Kleinman, D. L., and Young, L. R., "Display/Control Requirements for Automated VTOL Aircraft," NASA CR-158905, ASI-TR-76-39, Oct. 1976.

[18]McRuer, D. T., and Krendel, E. S., "Mathematical Models of Human Behavior," AGARDograph 188, Jan. 1984.

[19]Wierwille, W. W., and Connor, S. A., "Evaluation of 20 Workload Measures Using a Psychomotor Task in a Moving-Base Aircraft Simulator," *Human Factors,* Vol. 25, Feb. 1983, pp.1-16.

[20]Hess, R. A., "Effects of Time Delays of Systems Subject to Manual Control," *Journal of Guidance, Control, and Dynamics,* Vol. 7, No. 4, 1984, pp. 416-421.

[21]Hoh, R. H., Klein, R. H., and Johnson, W. A., "Development of an Integrated Configuration Management/Flight Director System for Piloted STOL Approaches," NASA TR-1015-4, Aug. 1977.

[22]Franklin, J. A., Innis, R. C., and Hardy, G. H., "Flight Evaluation of Stabilization and Command Augmentation System Concepts and Cockpit Displays During Approach and Landing of a Powered Lift STOL Aircraft," NASA TP-1551, 1980.

[23]Garg, S., and Schmidt, D. K., "Model-Based Analysis of Control/Display Interaction in the Hover Task," *Journal of Guidance, Control, and Dynamics,* Vol. 12, No. 3, 1989, pp. 342-350.

[24]Foster, J. D., Moralez, E. III, Franklin, J. A., and Schroeder, J. A., "Integrated Control and Display Research for Transition and Vertical Flight on the NASA V/STOL Research Aircraft (VSRA)," NASA TM-100029, Oct. 1987.